FOSSEE, IIT Bombay
OpenFOAM Research Migration Project
January 10, 2022

Prediction of Turbulence in Separated Flow using Asymmetric Diffuser Geometry

Divyesh Variya
FOSSEE Team, IIT Bombay

Synopsis

This research migration project aims to do numerical simulations of the turbulent flow in an asymmetric two-dimensional diffuser using `OpenFOAM foamExtend-4.1`. The geometry and mesh were defined using `blockMesh` utility. A steady-state, SIMPLE algorithm-based `simpleFoam` solver was used in the simulation. For accurate turbulence predictions, the $\kappa - \epsilon$ family, $\kappa - \omega$ and $\kappa - \omega SST$ turbulence models were used and compared with the experimental data. The analysis executed by Samy et. al. [1] using commercial CFD code `Fluent` was taken as a reference. The

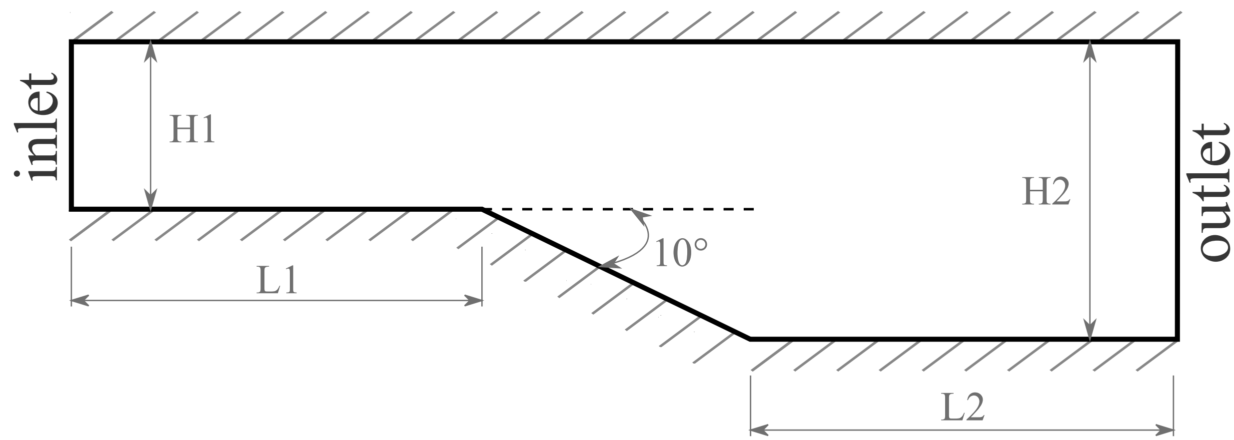

Figure 1: Geometry and Dimensions

dimensions of the geometry stated in the figure 1 are: $L1 = 60m$, $H1 = 2m$, $L2 = 70m$ and $H2 = 9.4m$. Flowing fluid is entering from inlet with velocity of $1.25m/s$ and exiting from outlet.

References

[1] Samy M. El-Behery and Mofreh H. Hamed. "A comparative study of turbulence models performance for separating flow in a planar asymmetric diffuser". In: *Computers & Fluids* 44.1 (2011), pp. 248–257. ISSN: 0045-7930. DOI: `https://doi.org/10.1016/j.compfluid.2011.01.009`. URL: `https://www.sciencedirect.com/science/article/pii/S0045793011000168`.

1 Introduction

In the reference paper [1], an asymmetric planar diffuser test case was analyzed to compare numerical results generated by various turbulence models against experimental data. A two-dimensional geometry is considered in the reference paper from data given in the test cases [9] [2]. The diffuser geometry given in fig. 1 can be divided into three sections: an inflow channel, the asymmetric diffuser, and an outflow channel. The inflow channel portion is sufficiently long to obtain fully developed turbulent channel flow. In order to capture flow separation in the diffuser and outflow channel, results of six different turbulence generated using commercial CFD code Fluent compared against experimental data. The turbulence model used in the reference paper is standard $\kappa - \epsilon$ model(SKE) [6], Low-Reynolds-number $\kappa - \epsilon$ model (LRNKE) [5], standard $\kappa - \omega$ model (SKW) [3], shear-stress transport $\kappa - \omega$ model (SST) [8], Reynolds stress model (RSM) [4], and $\nu^2 - f$ turbulence model (V2F) [7]. The reference study also did a grid conversion study with y^+ value of 30, 15, and 1. The pressure gradient, skin friction coefficient, velocity and turbulent kinetic energy values were compared to conclude.

2 Governing Equations and Models

To reproduce results generated by Samy [1], `OpenFOAM foamExtend-4.1` software was used. The Navier-Stokes equations for single-phase flows govern the simulation and are later compiled with 2-equation based turbulence models to capture turbulence in the flow. The governing continuity and momentum equations are given by:

2.1 Governing Equations

$$\nabla \cdot u = 0 \tag{1}$$

$$\nabla \cdot (u \otimes u) - \nabla \cdot R = -\nabla p + S_u \tag{2}$$

2.2 Turbulence Model

Several turbulence models are available in the `OpenFOAM foamExtend-4.1`. The five turbulence models (2-eqn. based) employed in this research migration project and compared. The turbulence models used are: standard $\kappa - \epsilon$ model [6], Realizable $\kappa - \epsilon$ model [10], RNG$\kappa - \epsilon$ [12], standard $\kappa - \omega$ model (SKW) [3], and shear-stress transport $\kappa - \omega$ model (SST) [8].

2.2.1 Standard $\kappa - \epsilon$ model

The $\kappa - \epsilon$ model is widely used and well described in the literature. In this model, flow is considered fully developed and assumed that the effects of molecular viscosity are negligible [6]. Hence, at the walls, the wall function approach is used.

$$\frac{\partial}{\partial t}(\rho\kappa) = \nabla \cdot (\rho D_\kappa \nabla\kappa) + P - \rho\epsilon \tag{3}$$

Where,
κ = Turbulent kinetic energy $[m^2 s^{-2}]$
D_κ = Effective diffusivity for $\kappa[-]$
P = Turbulent kinetic energy production rate $[m^2 s^{-3}]$
ϵ = Turbulent kinetic energy dissipation rate $[m^2 s^{-3}]$

$$\frac{\partial}{\partial t}(\rho\epsilon) = \nabla \cdot (\rho D_\epsilon \nabla \epsilon) + \frac{C_1 \epsilon}{\kappa}\left(P + C_3 \frac{2}{3}\kappa \nabla \cdot u\right) - C_2 \rho \frac{\epsilon^2}{\kappa} \tag{4}$$

Where,
D_ϵ = Effective diffusivity for $\epsilon[-]$
C_1 = Model coefficient $[-]$
C_2 = Model coefficient $[-]$

$$\nu_t = C_\mu \frac{\kappa^2}{\epsilon} \tag{5}$$

Where,
C_μ = Model coefficient for the turbulent viscosity $[-]$
ν_t = Turbulent viscosity $[m^2 s^{-1}]$

The model coefficients are
$C_\mu = 0.09;$ $C_1 = 1.44;$ $C_2 = 1.92;$ $C_{3,RDT} = 0.0;$ $\sigma_\kappa = 1.0;$ $\sigma_\epsilon = 1.3$

2.2.2 Realizable $\kappa - \epsilon$ model

The realizable $\kappa - \epsilon$ model [10] has increased popularity due to its improved performance over the standard $\kappa - \epsilon$ model. The model is similar to the standard $\kappa - \epsilon$ but improved with two aspects. First, it employs a different formulation of the transport equation for the dissipation rate derived from the transport equation for the mean-square vorticity fluctuations. Second, it uses a different eddy-viscosity formulation based on several realisability constraints for the turbulent Reynolds stresses. The C_μ is a function of local parameters rather than a constant value.

$$\frac{\partial}{\partial t}(\rho\kappa) = \nabla \cdot (\rho D_\kappa \nabla \kappa) + \rho G - \frac{2}{3}\rho(\nabla \cdot u)\kappa - \rho\epsilon + S_\kappa \tag{6}$$

$$\frac{\partial}{\partial t}(\rho\epsilon) = \nabla \cdot (\rho D_\epsilon \nabla \epsilon) + C_{1\epsilon}\rho|S|\epsilon - C_{2\epsilon}\rho\frac{\epsilon^2}{\kappa + (\nu\epsilon)^{0.5}} + S_\epsilon \tag{7}$$

$$\nu_t = C_\mu \frac{\kappa^2}{\epsilon} \tag{8}$$

$$C_{1\epsilon} = max[0.43, \frac{S \times \kappa}{S \times \kappa + 5\epsilon}] \tag{9}$$

$$C_\mu = \frac{1}{A_0 + A_s U * \frac{\kappa}{\epsilon}} \tag{10}$$

The model coefficients are
$A_0 = 4.0;$ $C_{2\epsilon} = 1.9;$ $\alpha_\kappa = 1;$ $\alpha_\epsilon = 0.83$

2.2.3 RNG $\kappa - \epsilon$ model

The RNG $\kappa - \epsilon$ model is a re-normalization group based $\kappa - \epsilon$ model. Over the years, multiple RNG $\kappa - \epsilon$ versions developed. The latest version developed by Yakhot and Smith [12] has a re-evaluation of the constant controlling the production of ϵ; and an additional production term in the ϵ equation which becomes significant in rapidly-distorted flows and flows removed from equilibrium.

$$\frac{\partial}{\partial t}(\rho\kappa) = \nabla \cdot (\rho D_\kappa \nabla \kappa) + P - \rho\epsilon \tag{11}$$

$$\frac{\partial}{\partial t}(\rho\epsilon) = \nabla \cdot (\rho D_\epsilon \nabla \epsilon) + \frac{C_1 \epsilon}{\kappa}\left(P + C_3 \frac{2}{3}\kappa \nabla \cdot u\right) - C_2 \rho \frac{\epsilon^2}{\kappa} \tag{12}$$

$$\nu_t = C_\mu \frac{\kappa^2}{\epsilon} \tag{13}$$

The model coefficients are
$C_\mu = 0.0845$; $C_1 = 1.42$; $C_2 = 1.68$; $\alpha\kappa = 1.39$; $\alpha\epsilon = 1.39$; $\beta = 0.012$

2.2.4 Standard $\kappa - \omega$ model

The standard $\kappa - \omega$ model has two popular versions[1988,2008] developed by Wilcox [3] [11]. The $\kappa - \omega$ version performs better in transitional flows and in flows with adverse pressure gradients. It is noticed that $\kappa - \omega$ model is numerically very stable, especially the low-Re version, as it tends to produce converged solutions more rapidly than the $\kappa - \epsilon$ family models. In 2008, Wilcox presented a revised $\kappa - \omega$ model that incorporates a cross-diffusion term, a stress-limiter modification to the eddy viscosity, and a vortex-stretching modification to the ω equation.

$$\frac{\partial}{\partial t}(\rho\kappa) = \nabla \cdot (\rho D_\kappa \nabla \kappa) + P - \rho\epsilon \tag{14}$$

$$\frac{\partial}{\partial t}(\rho\omega) = \nabla \cdot (\rho D_\omega \nabla \omega) + \sigma \nabla\kappa \nabla\omega \frac{\rho}{\omega} + \rho\omega \frac{C_{1\omega} P}{\kappa - C_{2\omega}\omega} \tag{15}$$

Model coefficients
$\sigma_\kappa = 1.67$; $\sigma_\omega = 2.0$; $C_\mu = 0.09$; $C_{1\omega} = 0.52$

2.2.5 Shear-stress transport $\kappa - \omega$ model

The shear-stress transport $\kappa - \omega$ model [8] uses the turbulent shear stress transport and offers improved flow separation predictions under adverse pressure gradients. It combined the capabilities of $\kappa - \omega$ turbulence model near walls and $\kappa - \epsilon$ model away from the walls.

$$\frac{\partial}{\partial t}(\rho\omega) = \nabla \cdot (\rho D_\omega \nabla \omega) + \frac{\rho\gamma G}{\nu} - \frac{2}{3}\rho\gamma\omega(\nabla \cdot u) - \rho\beta\omega^2 - \rho(F_1 - 1)CD_\kappa\omega + S_\omega \tag{16}$$

$$\frac{\partial}{\partial t}(\rho\kappa) = \nabla \cdot (\rho D_\kappa \nabla \kappa) + \rho G - \frac{2}{3}\rho(\nabla \cdot u)\kappa - \rho\beta * \omega\kappa + S_\kappa \tag{17}$$

$$\nu_t = a_1 \frac{\kappa}{max(a_1\omega, b_1 F_{23} S)} \tag{18}$$

Model coefficients
$\alpha\kappa 1 = 0.85$; $\alpha\kappa 2 = 1.0$; $\alpha\omega 1 = 0.5$; $\alpha\omega 2 = 0.856$; $\gamma_1 = 0.5532$; $\gamma_2 = 0.4403$
$\beta_1 = 0.075$; $\beta_2 = 0.0828$; $\beta^* = 0.09$; $a_1 = 0.31$; $c_1 = 10$

3 Simulation Procedure

3.1 Geometry and Mesh

The geometry presented in fig. 1 has three sections: an inlet, asymmetric diffuser and an outlet channel. The inlet channel is sufficiently long to generate a fully developed flow profile at the beginning of the diffuser. The asymmetric diffuser angle is 10 degrees. A 2-dimensional geometry has been considered in the study. Using `blockMesh` utility, geometry, and mesh defined with six

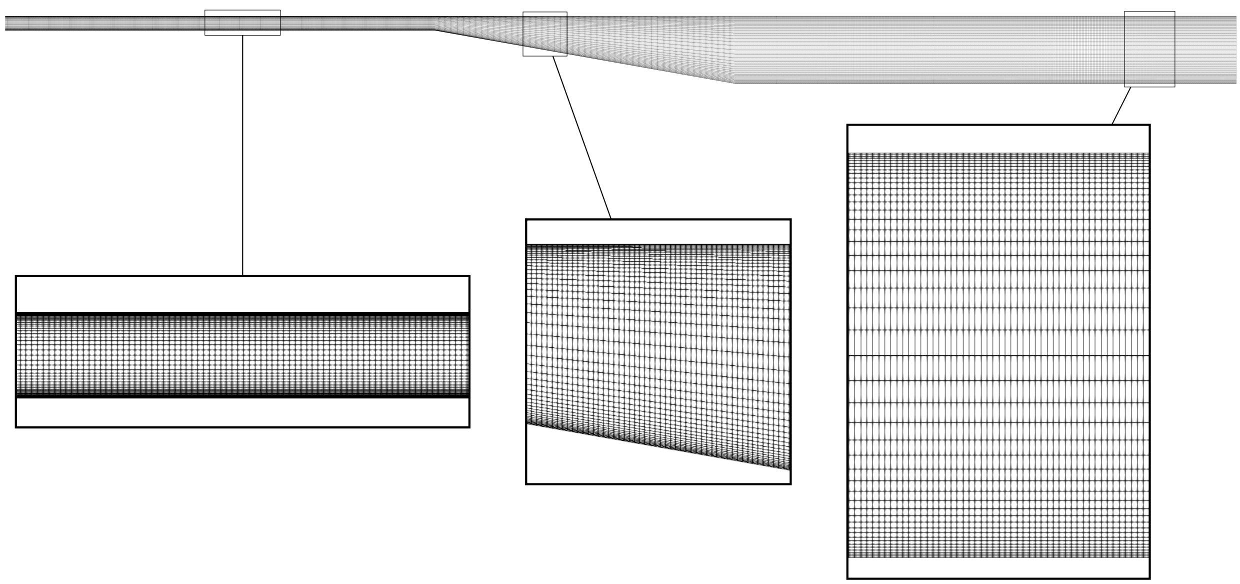

Figure 2: Computational grid

blocks. A structured grid consisting of 1300×46 cells in the stream-wise and wall-normal direction has been used. For refinement near the wall, expansion ratios 16 and 0.0625 were used for the top and bottom portions, as shown in fig. 2. The expansion ratio value kept y^+ value close to 1 in the simulation, as shown in fig. 3.

3.2 Initial and Boundary Conditions

There are four boundaries that required boundary conditions: An inlet, outlet, upperWall and lowerWall. The other two boundaries are front and back; that set as empty boundaries. At the inlet velocity, κ, ϵ, and ω are specified, as shown in table 1. At the walls, wall-function approach used for κ, ϵ, and ω. The turbulent viscosity(ν_t) value was calculated based on other parameters hence, kept

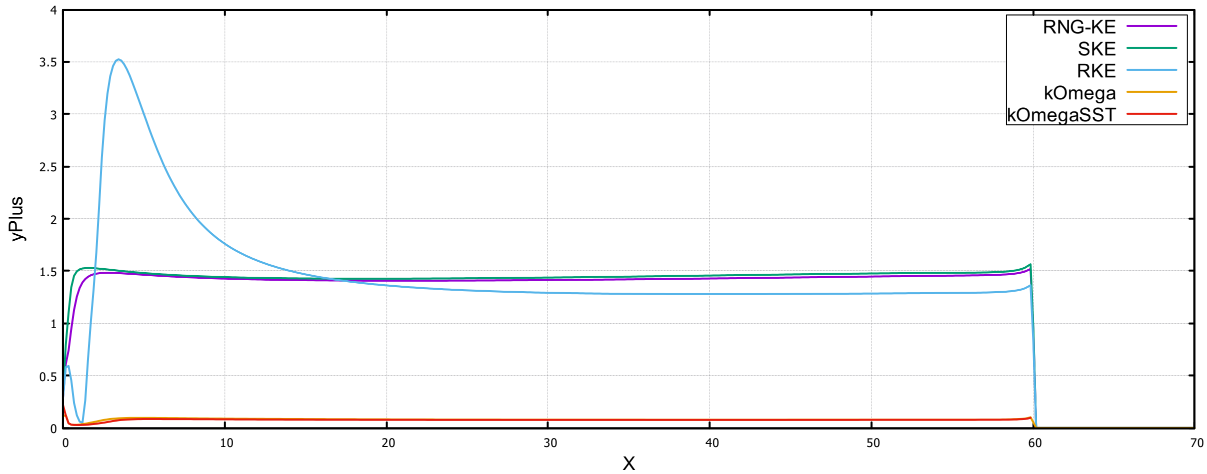

Figure 3: Y^+ comparison

calculated. The boundary condition data was taken from the experimental setup done by Obi [9] and Buice [2].

Table 1: Boundary condition

	Initial	inlet	outlet	walls
$U[m^2s^{-1}]$	0	1.25	ZG	noSlip
$p[m^2s^{-2}]$	0	ZG	0	ZG
$\kappa[m^2s^{-2}]$	1.8e-3	1.8e-3	ZG	kqRWallFunction
$\epsilon[m^2s^{-3}]$	9.63e-5	9.63e-5	ZG	epsilonWallFunction
$\omega[s^{-1}]$	0.5944	0.5944	ZG	omegaWallFunction
$\nu_t[m^2s^{-1}]$	0	calculated		

3.3 Solver

A steady-state for incompressible, turbulent flow-based `simpleFoam` solver is used to run governing equations in the discretized domain. The `simpleFoam` solver uses SIMPLE (Semi-Implicit Method for Pressure Linked Equations) algorithm to evaluate NS equations. The solver follows a segregated solution strategy. This means that the equations for each variable characterizing the system (the velocity u, the pressure p, and the variables characterizing turbulence) are solved sequentially. The solution of the preceding equations is inserted in the following equation.

For the convergence, conditional strategy used with 2000 maximum iterations or 10^5 convergence criteria. The standard $\kappa - \epsilon$ and RNG $\kappa - \epsilon$ cases converged at 1191 and 1226 iterations, respectively as shown in fig. 4a and 4b. The standard $\kappa - \omega$ and realizable $\kappa - \epsilon$ cases converged at 1536 and 1863 iterations, respectively as shown in fig. 4d and 4c. Whereas the shear-stress transport $\kappa - \omega$ case did not converge at given criteria untill 2000 iterations and stopped running, as shown in fig. 4e.

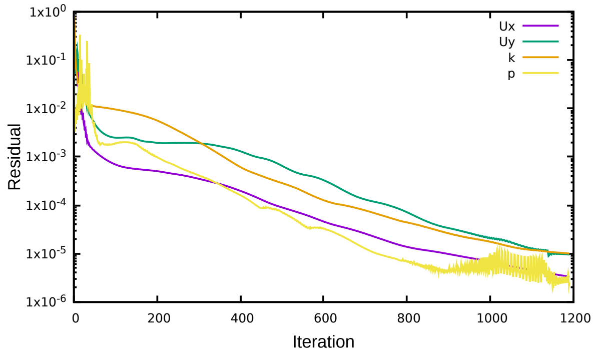

(a) Standard $\kappa - \epsilon$ model

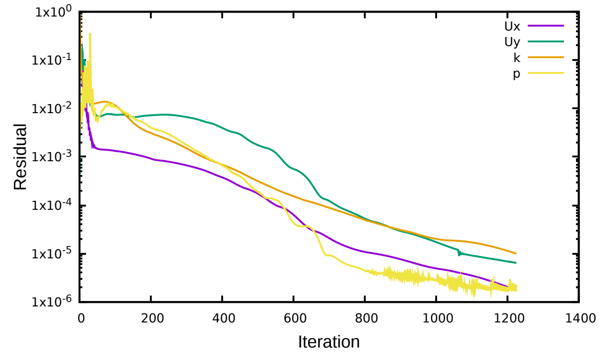

(b) RNG $\kappa - \epsilon$ model

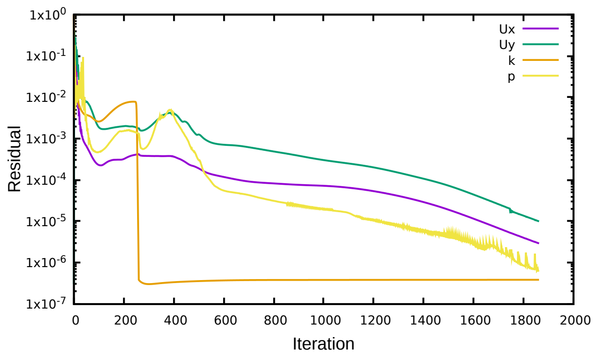

(c) Realizable $\kappa - \epsilon$ model

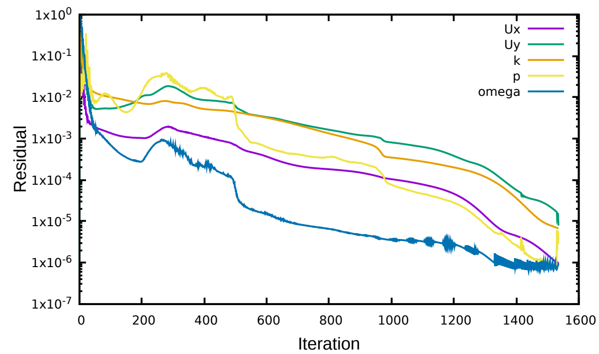

(d) Standard $\kappa - \omega$ model

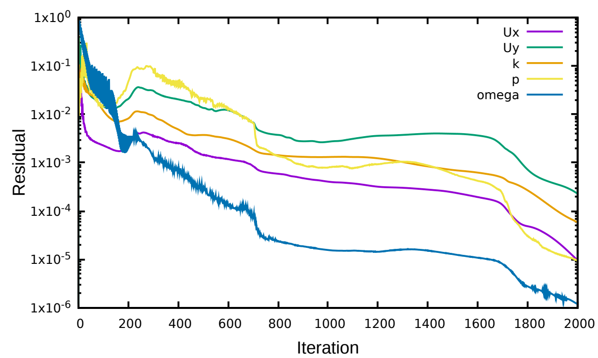

(e) Shear-stress transport $\kappa - \omega$ model

Figure 4: Residuals convergence

4 Results and Discussions

For the comparison of the results, pressure recovery coefficient(C_p), modified velocity(10*U+X-60), modified turbulent kinetic energy(500*κ+X-60), skin friction(C_f), and streamlines plotted. The results were compared with the experimental data or the reference paper [1].

Fig. 5compares pressure recovery coefficient over diffuser for different turbulence models used in the simulations. The results show that significant pressure increase occurs within the initial one-third of the diffuser, and Samy has observed the same [1]. However, the results of shear-stress transport $\kappa - \omega$ model in `OpenFOAM` did not match as discussed in the reference paper.

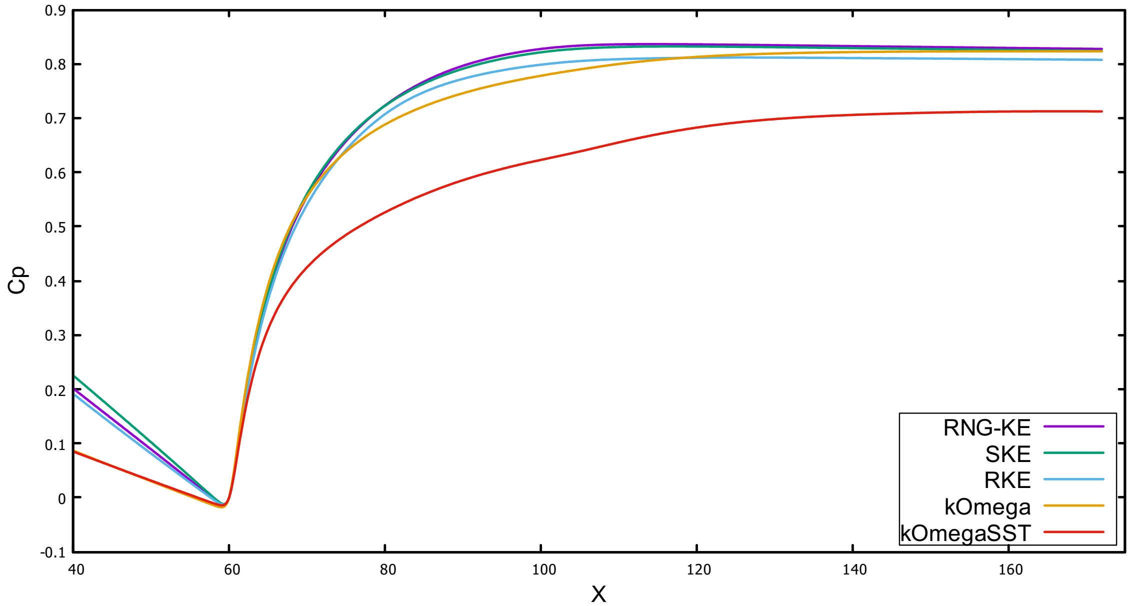

Figure 5: Pressure recovery coefficient comparison

The turbulent kinetic energy profile is presented in fig. 6 and 7. It can be seen that almost every model over-predicts the turbulent kinetic energy(TKE) in the diffuser section. However, $\kappa - \epsilon$ family models under-predicts TKE in the expanded channel section. Whereas $\kappa - \omega$ family models give more promising results near the top-wall and in the expanded channel section.

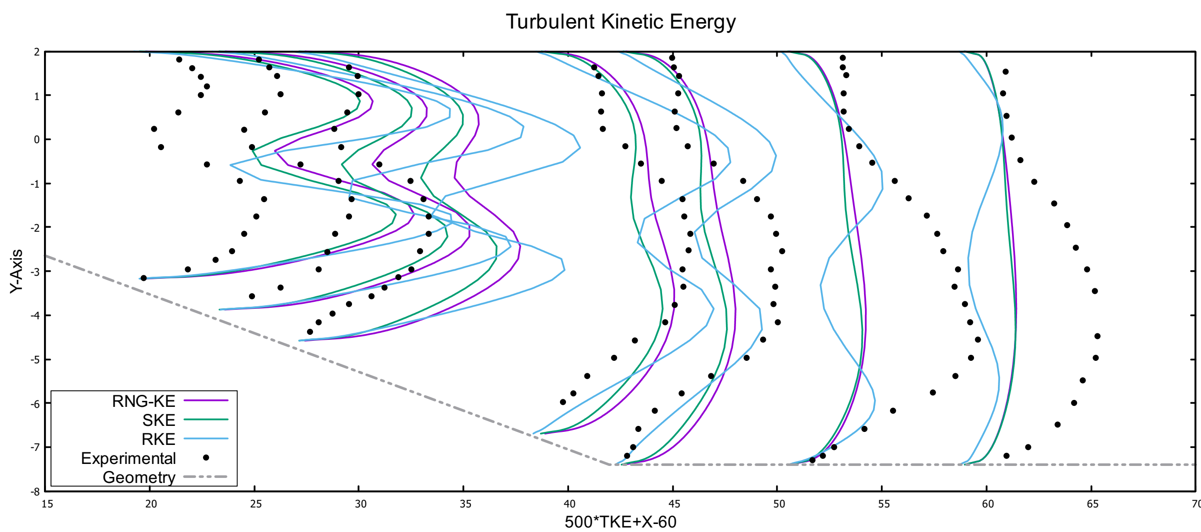

Figure 6: Turbulent Kinetic Energy κ: $\kappa - \epsilon$ family models

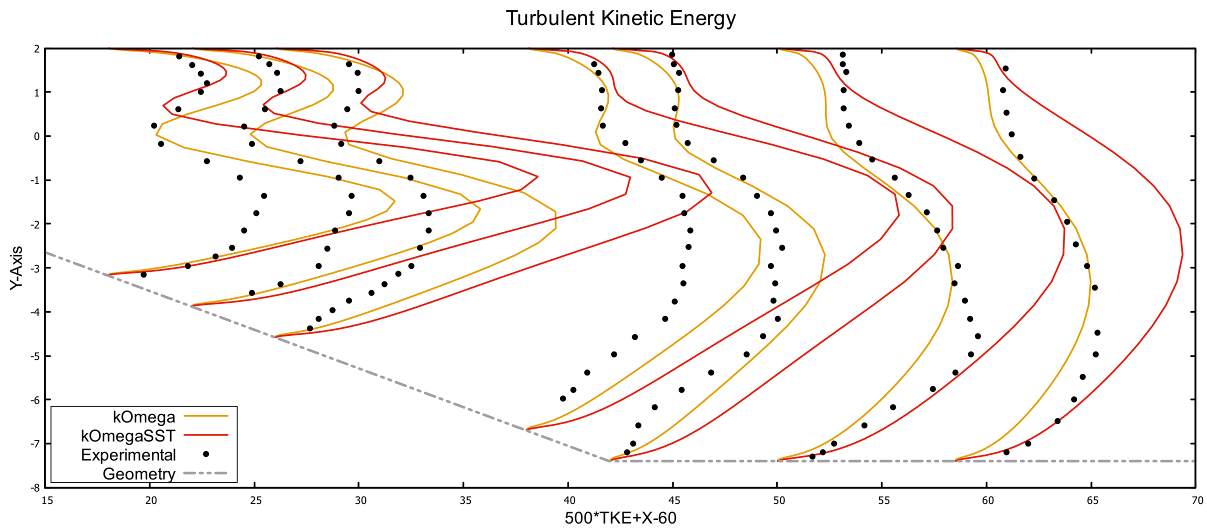

Figure 7: Turbulent Kinetic Energy κ: $\kappa - \omega$ and $\kappa - \omega$ SST models

In fig. 8 and 9, velocity is plotted in the modified form and compared with the experimental data. The results indicate that SST and SKW models predict the axial velocity profiles well. Whereas the entire $\kappa - \epsilon$ family models fail to predict the velocity in the separation zone. However, the Realizable $\kappa - \epsilon$ model captures velocity very well near the top-wall region. The same has been observed by Samy [1].

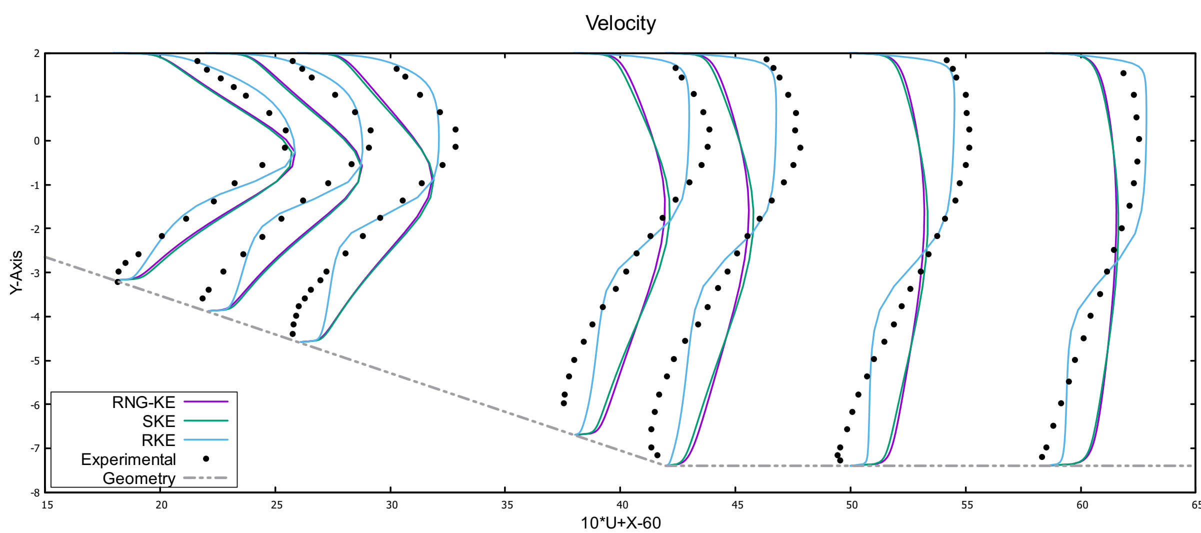

Figure 8: Velocity profile: $\kappa - \epsilon$ family models

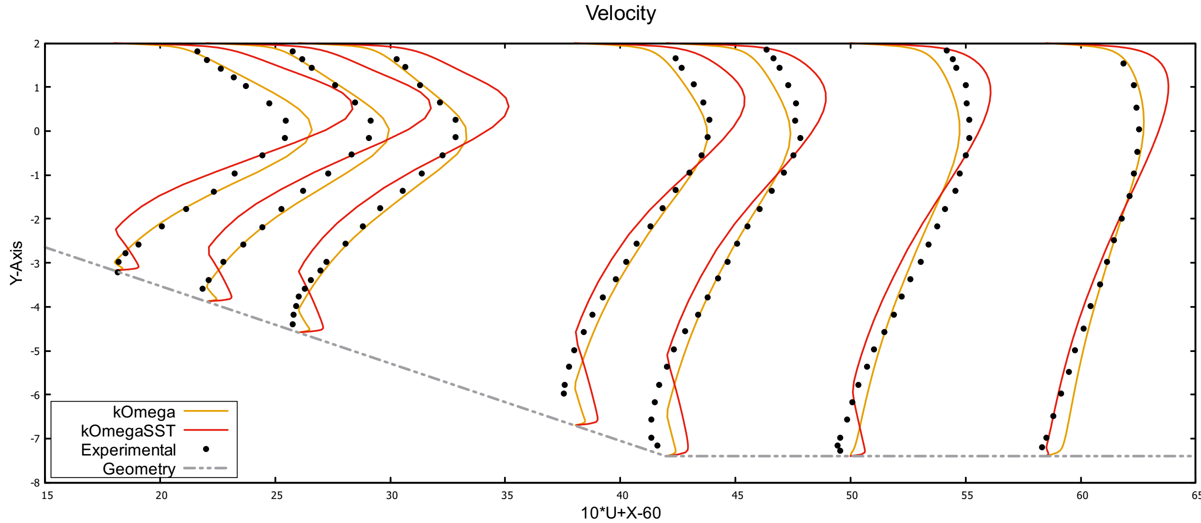

Figure 9: Velocity profile: $\kappa - \omega$ and $\kappa - \omega$ SST models

The skin friction coefficients on both the top and bottom wall for different turbulence models used in the study are presented in fig. 10. From the plots, it is notable that there is a significant difference between experimental and numerical data. Though, KOSST and SKO models follow the trend. But entire $\kappa - \epsilon$ family fails to predict the skin friction coefficient, and the same has been noticed in the reference paper.

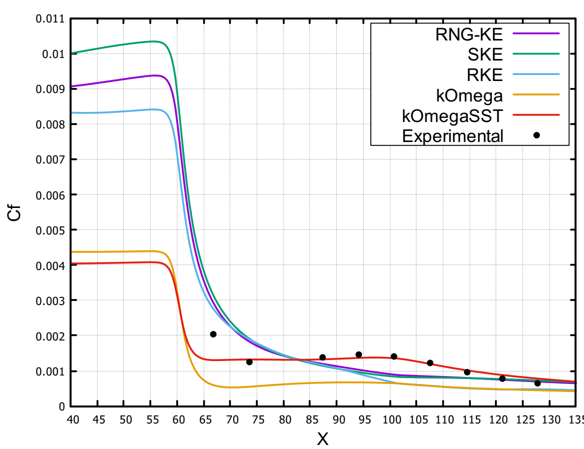

(a) Top wall

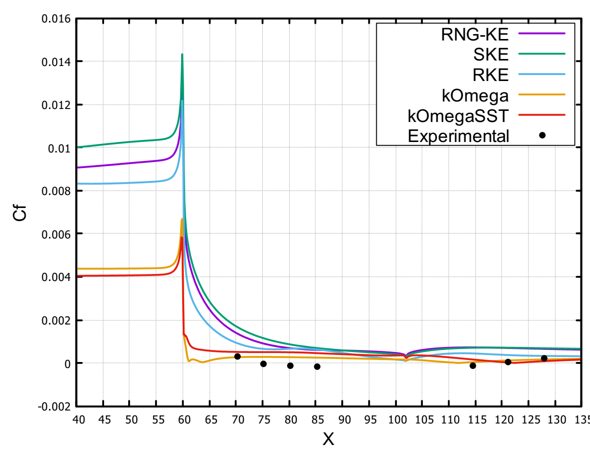

(b) Bottom wall

Figure 10: Skin friction coefficient C_f

Fig. 11 shows streamlines for different turbulence models at steady-state. The flow separation is noticeable in the standard $\kappa - \omega$ and shear-stress transport $\kappa - \omega$ model. The $\kappa - \epsilon$ family models fail to generate a separation bubble in the diffuser section.

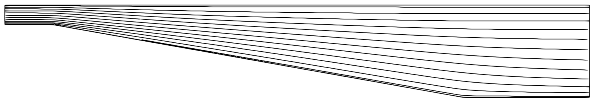

(a) Standard $\kappa - \epsilon$ model

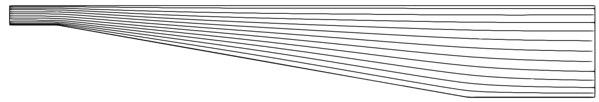

(b) RNG $\kappa - \epsilon$ model

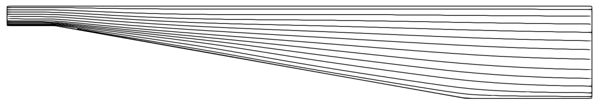

(c) Realizable $\kappa - \epsilon$ model

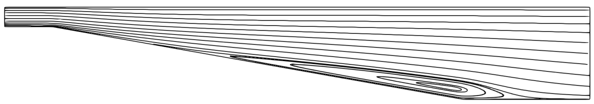

(d) Standard $\kappa - \omega$ model

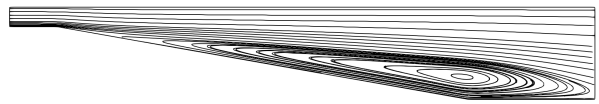

(e) Shear-stress transport $\kappa - \omega$ model

Figure 11: Streamline plots

References

[1] Samy M. El-Behery and Mofreh H. Hamed. "A comparative study of turbulence models performance for separating flow in a planar asymmetric diffuser". In: *Computers & Fluids* 44.1 (2011), pp. 248–257. ISSN: 0045-7930. DOI: `https://doi.org/10.1016/j.compfluid.2011.01.009`. URL: `https://www.sciencedirect.com/science/article/pii/S0045793011000168`.

[2] Carl U Buice. *Experimental investigation of flow through an asymmetric plane diffuser*. Stanford University, 1997.

[3] Wilcox DC. *Turbulence modeling for CFD*. La Canada, California: DCW Industries, 1998.

[4] B. E. (Brian Edward) Launder. *Lectures in mathematical models of turbulence / B. E. Launder and D. B. Spalding.* eng. London: Academic Press, 1972.

[5] B.E. Launder and B.I. Sharma. "Application of the energy-dissipation model of turbulence to the calculation of flow near a spinning disc". In: *Letters in Heat and Mass Transfer* 1.2 (1974), pp. 131–137. ISSN: 0094-4548. DOI: `https://doi.org/10.1016/0094-4548(74)90150-7`. URL: `https://www.sciencedirect.com/science/article/pii/0094454874901507`.

[6] B.E. Launder and D.B. Spalding. "The numerical computation of turbulent flows". In: *Computer Methods in Applied Mechanics and Engineering* 3.2 (1974), pp. 269–289. ISSN: 0045-7825. DOI: `https://doi.org/10.1016/0045-7825(74)90029-2`. URL: `https://www.sciencedirect.com/science/article/pii/0045782574900292`.

[7] Fue-Sang Lien and Georgi Kalitzin. "Computations of transonic flow with the v2–f turbulence model". In: *International Journal of Heat and Fluid Flow* 22.1 (2001), pp. 53–61. ISSN: 0142-727X. DOI: `https://doi.org/10.1016/S0142-727X(00)00073-4`. URL: `https://www.sciencedirect.com/science/article/pii/S0142727X00000734`.

[8] Florian R. Menter. "Two-equation eddy-viscosity turbulence models for engineering applications". In: *AIAA Journal* 32 (1994), pp. 1598–1605.

[9] Obi S, Aoki K, and Masuda S. "Experimental and computational study of turbulent separating flow in an asymmetric plane diffuser". In: *Ninth symposium on turbulent shear flows* (1993), pp. 305-1–4.

[10] Tsan-Hsing Shih et al. "A new $\kappa - \epsilon$ eddy viscosity model for high reynolds number turbulent flows". In: *Computers & Fluids* 24.3 (1995), pp. 227–238. ISSN: 0045-7930. DOI: `https://doi.org/10.1016/0045-7930(94)00032-T`. URL: `https://www.sciencedirect.com/science/article/pii/004579309400032T`.

[11] David C. Wilcox. "Formulation of the k-w Turbulence Model Revisited". In: *AIAA Journal* 46.11 (2008), pp. 2823–2838. DOI: `10.2514/1.36541`. eprint: `https://doi.org/10.2514/1.36541`. URL: `https://doi.org/10.2514/1.36541`.

[12] V. Yakhot et al. "Development of turbulence models for shear flows by a double expansion technique". In: *Physics of Fluids A: Fluid Dynamics* 4.7 (1992), pp. 1510–1520. DOI: `10.1063/1.858424`. eprint: `https://doi.org/10.1063/1.858424`. URL: `https://doi.org/10.1063/1.858424`.

DISCLAIMER: This project reproduces the results from an existing work, which has been acknowledged in the report. Any query related to the original work should not be directed to the contributor of this project.